Comparative Visual Analysis of Pelvic Organ Segmentations

O. Reiter[1], M. Breeuwer[2,3], M.E. Gröller[1,4], R.G. Raidou[1]

[1]TU Wien, Austria, [2]Eindhoven University of Technology, the Netherlands, [3]Philips Healthcare Best, the Netherlands, [4]VRVis Research Center, Austria

Abstract

In prostate cancer treatment, automatic segmentations of the pelvic organs are often used as input to radiotherapy planning systems. However, natural anatomical variability of the involved organs is a common reason, for which segmentation algorithms fail, introducing errors in the radiotherapy treatment procedure, as well. Understanding how the shape and size of these organs affect the accuracy of segmentation is of major importance for developers of segmentation algorithms. However, current means of exploration and analysis provide limited insight. In this work, we discuss the design and implementation of a web-based framework, which enables easy exploration and detailed analysis of shape variability, and allows the intended users – i.e., segmentation experts – to generate hypotheses in relation to the performance of the involved algorithms. Our proposed approach was tested with segmentation meshes from a small cohort of 17 patients. Each mesh consists of four pelvic organs and two organ interfaces, which are labeled and have per-triangle correspondences. A usage scenario and an initial informal evaluation with a segmentation expert demonstrate that our framework allows the developers of the algorithms to quickly identify inaccurately segmented organs and to deliberate about the relation of variability to anatomical features and segmentation quality.

CCS Concepts

•*Human-centered computing* → *Visual analytics;* •*Applied computing* → *Life and medical sciences;*

1. Introduction

In radiotherapy treatment of prostate cancer, a careful plan is conducted prior to the administration of the irradiation dose [Was15]. Common treatment planning systems use as input segmentations of the involved pelvic organs, such as the prostate, rectum, seminal vesicles and bladder. This is done with the purpose of preserving healthy tissues adjacent to the tumors to be treated. However, the administered high irradiation dose could also damage these healthy tissues, if the latter have not been accurately segmented. As manual segmentation of the pelvic organs is time consuming, automatic approaches are often preferred [SBV*13], even if they may produce suboptimal results. Therefore, segmentation experts are continuously working on improving their algorithms.

Evaluating segmentation outcomes is often simple. However, understanding when and why an algorithm fails remains a major problem [RMB*16]. Researchers working on the development of segmentation algorithms have a hypothesis that the shape and size of the involved organs may play an important role in the performance of their algorithms [CLR11]. Pelvic organs are subject to high anatomical variability – especially the bladder and the rectum, which are flexible soft tissues, prone to volume changes due to changes in their filling [Was15]. Therefore, it is interesting to explore the relation between the natural anatomical variability of pelvic organs with respect to algorithmic performances, and in particular, within cohorts of patients. The exploration of this relation is currently not possible with the existing means of analysis.

The *contribution* of this work is the design and implementation of a web-based framework for the visual exploration and analysis of shape variability in pelvic organs and its impact on segmentation accuracy. The framework is meant to be used by segmentation experts and to enable them to perform two main tasks:

- **(T1)** Quantification and visualization of the shape variability of *one or more pelvic organs, at the same time*.
- **(T2)** Comparative visualization of *several pelvic organ segmentations* in a cohort of patients, *simultaneously*.

2. Related Work

Recently, Raidou et al. [RMB*16] proposed a visualization framework for the *exploration and analysis of segmentation outcomes* in a cohort of subjects. This work covers the detailed assessment of segmentations, but does not extend to shape space analysis. Other frameworks for the analysis of the impact of parameters on segmentation algorithm outcomes were designed by Torsney et al. [TWSM*11] and Fröhler et al. [FMH16].

Several techniques for *visualizing shape spaces* and comparing shapes based on their similarity have been proposed in the past. Busking et al. [BBP10] employed space scatterplots linked to shape evolution views. This was later extended by Kirschner et al. [KBW11], also to non-Gaussian shape distributions. Von Landesberger et al. [vLBK*13, vLBB15] have also proposed tools to incorporate multiple shape space dimensions, to transform them interactively, and to allow the user to explore global information about the examined population. Hermann et al. proposed strategies to find trait vectors for the respective best separating axes
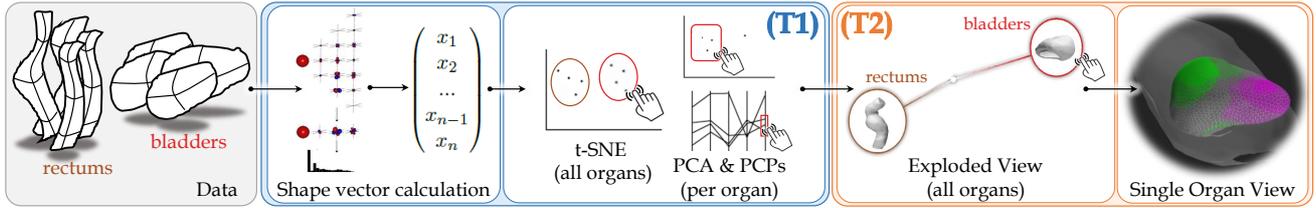
Figure 1: *Workflow of our proposed approach with the two main tasks* **(T1, T2)** *that it fulfills.*

within PCA plots [HSK11]. They later proposed other strategies for the quantification and understanding of shape variation and co-variance [HSSK14], which were extended to shape space navigation and visualization techniques [HK15]. Finally, Klemm et al. [KLR*13] proposed tools for the exploration of spines, based on clustering using multiple distance measures.

Comparative visualization relates to the visual evaluation of at least two subjects, with respect to each other [KCK17]. Busking et al. [BBF*11] proposed visualizations for the comparison of two surfaces, while Alabi et al. [AWH*12] proposed side-by-side comparison of 3D volumes. For mesh comparison, MeshLab [CCR08] and PolyMeCo [SMS09] were proposed, but they are also restricted to pairwise comparisons. Multiple subject comparison was only recently addressed by Schmidt et al. [SPA*14].

In *comparison to previous related approaches*, our specific application requires a solution that can deal with multiple, differently shaped organs, at the same time. Thus, new ways to analyze shape variability at a single- and multi-organ level have to be provided. This stands also for the visual comparison of the segmentation outcomes, which should address and display multiple organ classes from multiple patients, simultaneously. To the best of our knowledge, employing a visual analytics system to explore and analyze organ shape and size variability – especially, for a multitude of organs, at the same time – has not been proposed before.

3. Comparative Visual Analysis of Pelvic Organs

We propose a web-based framework that provides: (i) a way to *quantify and visualize the shape variability* of different pelvic organs **(T1)** and (ii) a strategy to *visualize multiple organs from multiple patients* in a single summarized view **(T2)**. The workflow of our approach is depicted in Figure 1.

(T1) Quantification and Visualization of Organ Variability — Our available segmentation data were provided as triangle meshes, where pelvic organs are labeled and have per-triangle correspondences. As a first step, shape features have to be extracted using a *suitable shape descriptor* and have to be compared with an *adequate metric*. Suitable descriptors, in our case, should provide translation and rotation invariance – but not scale, as the size of the organs is also expected to influence the segmentation outcome. A fast, yet precise, option is to employ a spherical harmonics-based descriptor [KFR03]. Other shape descriptors taken into account were 3D Zernike Descriptors [NK03], but they were discarded due to complexity reasons.

To employ shape descriptors based on *spherical harmonics*, a spherical function has to be determined. We selected a function that employs the distance to the centroid of the shapes at hand. The defined spherical function is then decomposed into its harmonics. The resulting descriptor consists of the L_2-norm of the accumulated coefficients of each frequency, which creates a rotation invariant representation. As the computation of the Legendre polynomials employed in the spherical harmonics approach is expensive for high orders, we decided to restrict the polynomials and, consequently the shape descriptor, to the 7th order. For a detailed description of our approach, we refer to our previous work [Rei18].

Having computed the descriptors for the available shapes, we also need to be able to compare them. For this, the L_2-difference was considered to be a suitable metric, as it is very commonly employed also within the spherical harmonics approach. The L_2-difference of the harmonic representation is a lower bound of the L_2-difference over all orientations of the spherical function. Our choices, so far, entail several limitations with respect to shape identification and comparison. These could be tackled by alternatives, such as Procrustes analysis [Goo91] or bi-spectrum based features [Kon08]. Yet, for the available organs and for the specific application, our current choices are regarded to be sufficient and the proposed alternatives are left as directions for future work.

The result of the previous step is an 8D (due to the 7th order) shape description vector. Since this vector cannot be visualized directly, it has to be converted into a lower dimensional space. At this point, we decided to incorporate two well-known *dimensionality reduction techniques*: PCA and t-SNE [MH08]. The reason for the integrated use of PCA and t-SNE is to combine their inherent properties. PCA is suitable for determining the variance within one organ class, but it does not discriminate well between classes. For the latter, t-SNE is more appropriate, due to its non-linear nature that facilitates between-class data separation. Both techniques are fast in computation time and their results can be easily visualized in a *2D scatterplot view* to facilitate interaction, outlier detection and visual cluster identification. This is depicted in Figure 2, where we initially employ t-SNE to differentiate between the different organ classes indicated by distinct colors. Subsequently, we conduct a PCA for each class of organs (either bladders or rectums). The colors for the organ classes are propagated from the t-SNE plot to the other representations for easier linking between views.

To provide access to the entire 8D space of the shape descriptor vectors, we additionally employ a *Parallel Coordinates Plot* (PCP) [Ins85]. PCPs are very suitable for the detection of patterns beyond 2D and for the easier identification of outliers, as depicted in Figure 2 for two different organs. In our application, PCPs enable the user to identify the frequencies that compose a shape and to compare them easily to those of other organs. *Brushing and linking*
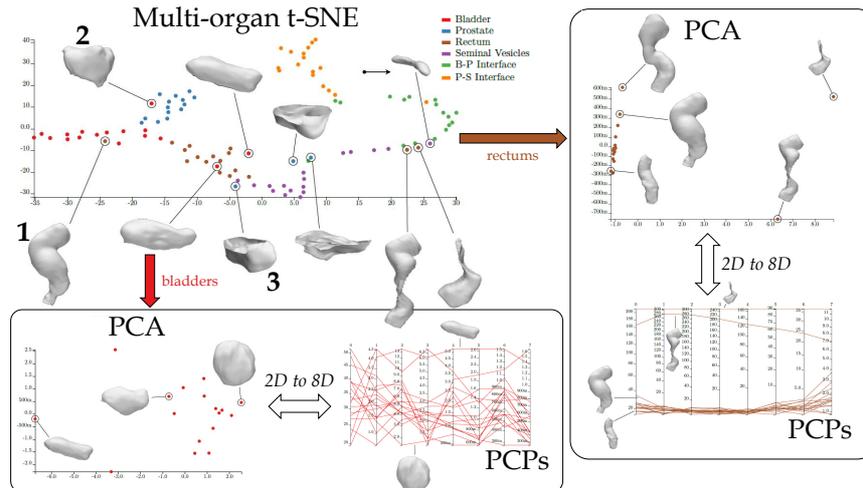
Figure 2: *Schematic depiction of the usage of dimensionality reduction techniques (PCA for single organs, t-SNE for multiple organs) of the shape descriptor vectors to facilitate interaction, outlier detection, and visual cluster identification in two dimensional scatterplots. PCPs provide additional access to the entire high-dimensional (8D) space of the shape descriptor vectors.*

between the PCA, t-SNE, and PCP views facilitates data analysis and sense-making. *Selection* of one or more data points in each of these plots links to the second task and to a view on the respective mesh segmentations, as described in the following subsection. The plots color scheme follows the guidelines from ColorBrewer.

(T2) Comparative Visualization of Multiple Pelvic Organs — The second component is linked to the first component of the framework. When the user performs a selection of one or more data points in the PCA, t-SNE, or PCP, a summarized view of the respective meshes is displayed. We will refer to it as *exploded view* and it was inspired and based on the previous work of Balabanian et al. [BVG10]. This view can be seen in Figure 3, for all the cohort organs. Our conceptual idea behind this undirected graph metaphor is to display multiple organs in a common representation – still, separated from each other. The exploded view aggregates all information of the organ shapes, but it also preserves to a certain extent anatomical context, the relative position of each organ to the rest, and adjacency to other organs or interfaces. Within the nodes of the graph, we display the median shape of the current selection for each organ. Adjacent organs are visually connected with edges, while disconnected components are connected to a white dot to indicate the existence of an in-between space. The colors of the circles enclosing each organ are the same as in the views of the first task, and the sizes are dictated by the sizes of the respective organs.

To compare local differences, the user can click on the node corresponding to one organ in the exploded view and obtain a *detail-on-demand view*. This view displays the median shape of the organ under exploration, but with some additional attributes. First of all, we incorporate and display information about the range of organ shapes that were selected. This is shown with a ghosted envelope of the maximum shape of the organ, as presented in Figure 3 for two different organs (bladders and rectums). Additionally, to encode information at each triangle position that indicates the number of members located on the outside or the inside of the median shape, we employ a diverging green(outside)-to-purple(inside) col-

ormap. The color scheme has been selected using guidelines from Rheingans [Rhe00]. Moreover, the per-triangle variance with respect to the median shape is also included in the view in the form of dot glyphs. The variance is encoded to the glyph opacity, with high opacity indicating high variance. For the design of the glyphs, we followed guidelines proposed by Borgo et al. [BKC*13]. Drilling down from a global to a local view is expected to enable users to understand how the shape of one or more organs changes within a cohort of patients, with as little as possible clutter. Previous approaches enabled the exploration of single organs only, but with our strategy, several organs can be explored simultaneously.

Implementation — The web-based application is implemented in Javascript. It makes use of D3.js for the visualizations of the first task and three.js, which uses WebGL, for the comparative visualizations of the second task. For the implementation of the spherical harmonics descriptors we employed the Spherical-Harmonic-Transform-JS library and functionality from Numeric Javascript.

4. Results and Evaluation

In this section, we present results that can be achieved with the use of our proposed approach in a usage scenario, as well as initial findings from an informal evaluation with a segmentation expert. Additional usage scenarios can be found in [Rei18].

Usage Scenario — We begin the exploration of our usage scenario, by loading all the available segmented data, with the four organs and their interfaces, from 17 patients. The shape descriptors are computed per organ for each patient. Then, the respective dimensionality reduction techniques are employed to reduce the 8D space of the shape descriptor to 2D. The top part of Figure 2 shows the t-SNE computed for all organs of the data set. The selected data points correspond to organs grouped within the wrong class. Further examination of the respective meshes in the exploded view shows that these organs look more similar to the organs of the neighboring data points. Starting from left to right, there is a rectum (brown point 1) within the class of bladders (red points), prob-
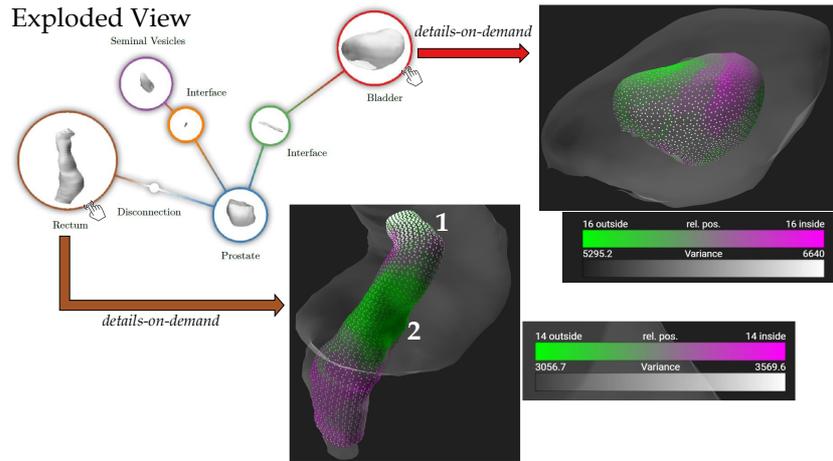
Figure 3: *Schematic depiction of the usage of the exploded view that visualizes several organs simultaneously and enables drilling down to single organs (here, bladders and rectums), to understand their respective shape variability.*

ably because of its small size. The bladder (red point 2) located among prostates (blue points) has also an unusual shape. Probably, it fits within this class because of similar size and slightly increased higher frequencies, as seen in the respective PCP. The prostate (blue point 3) located at the bottom of the t-SNE plot is also misclassified. An inspection of its shape shows that most probably the segmentation algorithm failed and the resulting segmentation was classified within the seminal vesicles class (purple points).

A local analysis of the shapes can be done in the per-organ PCA and PCP. The right side of Figure 2 shows the exploration of all rectums, only. The vertical component of the PCA plot of the rectums corresponds to the size of the organs. At the right end of this plot, there are two outliers with a rather unusual rectum shape, which are also visible in the PCP. The bottom part of Figure 2 shows the exploration of all bladders, only. The components of this PCA plot correspond to size and roundness. The PCP shows two vectors with higher values at high orders, which correspond to outliers both in the PCA plot and the initial t-SNE plot, due to their "flat" unusual shape – probably, a result of mis-segmentation.

For the second task, the exploded view is useful for comparing different organs at the same time, and their relative positions to each other (Figure 3, top). The detail-on-demand view aims at comparing a single organ type – in our case, bladders and rectums separately (Figure 3, right and bottom respectively). For the rectums, we perform a selection of all-but-outliers. Looking at the color encoding on the median shape of the selected organs, as well as the ghosted envelope (biggest rectum shape within the selection), the high variability in bending and size of this organ becomes obvious. The triangle positions at the top of the organ (marked with 1) have a higher variance than the middle and bottom, maybe because these parts expand more due to rectal filling. The area of lowest variance is at the back side of the rectum (marked with 2), where the spine restricts enlargement. Also in the bladders there is a high variability in shape and size, as depicted at the right side of Figure 3. These findings agree with the quantitative assessment conducted by Raidou et al. [RMB*16] on the same cohort data.

Evaluation — We conducted an initial informal evaluation with a senior scientist at Philips Healthcare, working in the field of segmentation for more than 25 years. The previously presented usage scenario was used to illustrate the functionality and to show some initial results. The employed cohort data were already known to the evaluator. During the demonstration, we documented the opinion of the evaluator, who commented that our framework is an easy to learn and easy to understand approach for analyzing the influence of organ shape variability on the performance of segmentation algorithms. He observed that the framework could be extended with views, showing the images on which the segmentations were performed and the organ delineations. He also remarked that it could be connected to an actual quantitative assessment of the segmentation outcome. All in all, the framework was regarded very positively, but a more detailed evaluation would need to be conducted.

5. Conclusions and Future Work

Our proposed framework allows segmentation experts to quickly quantify and visualize the shape variability of one or more pelvic organs, at the same time. It also enables the comparative analysis of several pelvic organ segmentations, in a single view. Directions for future work include the improvement of the employed shape descriptor, which deals best with round organs. An additional connection of our work with an actual assessment of segmentation outcome quality [RMB*16], would be a nice extension. It would provide further insight in how segmentation algorithms work and on how to improve them. Finally, our approach could also be used in other applications, where an exploration and analysis of shape features and shape variability is needed. It can also be used or extended for comparison of the variability in the outcomes from different (parametrizations of) segmentation algorithms.

References

[AWH*12] ALABI O. S., WU X., HARTER J. M., PHADKE M., PINTO L., PETERSEN H., BASS S., KEIFER M., ZHONG S., HEALEY C., ET AL.: Comparative visualization of ensembles using ensemble surface slicing. In *Proceedings of SPIE* (Jan 2012), vol. 8294, NIH Public Access. 2

[BBF*11] BUSKING S., BOTHA C. P., FERRARINI L., MILLES J., POST F. H.: Image-based rendering of intersecting surfaces for dynamic comparative visualization. *The Visual Computer 27*, 5 (2011), 347–363. 2

[BBP10] BUSKING S., BOTHA C. P., POST F. H.: Dynamic multi-view exploration of shape spaces. *Computer Graphics Forum 29*, 3 (2010), 973–982. 1

[BKC*13] BORGO R., KEHRER J., CHUNG D. H., MAGUIRE E., LARAMEE R. S., HAUSER H., WARD M., CHEN M.: Glyph-based visualization: Foundations, design guidelines, techniques and applications. *Eurographics State of the Art Reports* (May 2013), 39–63. 3

[BVG10] BALABANIAN J.-P., VIOLA I., GRÖLLER E.: Interactive illustrative visualization of hierarchical volume data. In *Proceedings of Graphics Interface 2010* (2010), Canadian Information Processing Society, pp. 137–144. 3

[CCR08] CIGNONI P., CORSINI M., RANZUGLIA G.: MeshLab: An open-source 3D mesh processing system. *Ercim news 73*, 45-46 (2008), 6. 2

[CLR11] CHEN S., LOVELOCK D. M., RADKE R. J.: Segmenting the prostate and rectum in CT imagery using anatomical constraints. *Medical Image Analysis 15*, 1 (2011), 1 – 11. 1

[FMH16] FRÖHLER B., MÖLLER T., HEINZL C.: GEMSe: Visualization-Guided Exploration of Multi-channel Segmentation Algorithms. *Computer Graphics Forum 35*, 3 (2016). 1

[Goo91] GOODALL C.: Procrustes methods in the statistical analysis of shape. *Journal of the Royal Statistical Society* (1991), 285–339. 2

[HK15] HERMANN M., KLEIN R.: A visual analytics perspective on shape analysis: State of the art and future prospects. *Computers & Graphics 53*, Part A (2015), 63 – 71. 40 years of Computer Graphics in Darmstadt. 2

[HSK11] HERMANN M., SCHUNKE A. C., KLEIN R.: Semantically steered visual analysis of highly detailed morphometric shape spaces. In *2011 IEEE Symposium on Biological Data Visualization (BioVis).* (Oct 2011), pp. 151–158. 2

[HSSK14] HERMANN M., SCHUNKE A. C., SCHULTZ T., KLEIN R.: A visual analytics approach to study anatomic covariation. In *2014 IEEE Pacific Visualization Symposium* (March 2014), pp. 161–168. 2

[Ins85] INSELBERG A.: The plane with parallel coordinates. *The Visual Computer 1*, 2 (1985), 69–91. 2

[KBW11] KIRSCHNER M., BECKER M., WESARG S.: *3D Active Shape Model Segmentation with Nonlinear Shape Priors.* Springer Berlin Heidelberg, Berlin, Heidelberg, 2011, pp. 492–499. 1

[KCK17] KIM K., CARLIS J. V., KEEFE D. F.: Comparison techniques utilized in spatial 3D and 4D data visualizations: A survey and future directions. *Computers & Graphics 67*, Supplement C (2017), 138 – 147. 2

[KFR03] KAZHDAN M., FUNKHOUSER T., RUSINKIEWICZ S.: Rotation invariant spherical harmonic representation of 3D shape descriptors. In *Symposium on geometry processing* (2003), vol. 6, pp. 156–164. 2

[KLR*13] KLEMM P., LAWONN K., RAK M., PREIM B., TÖNNIES K. D., HEGENSCHEID K., VÖLZKE H., OELTZE S.: Visualization and analysis of lumbar spine canal variability in cohort study data. In *VMV (Vision, Modeling and Visualization)* (2013), pp. 121–128. 2

[Kon08] KONDOR I. R.: *Group theoretical methods in machine learning.* Columbia University, 2008. 2

[MH08] MAATEN L. V. D., HINTON G.: Visualizing Data using t-SNE. *Journal of Machine Learning Research 9*, Nov (2008), 2579–2605. 2

[NK03] NOVOTNI M., KLEIN R.: 3D Zernike Descriptors for Content Based Shape Retrieval. In *Proceedings of the Eighth ACM Symposium on Solid Modeling and Applications* (New York, NY, USA, 2003), SM '03, ACM, pp. 216–225. 2

[Rei18] REITER O.: *Comparative Visualization of Pelvic Organ Segmentations.* Master's thesis, Institute of Visual Computing & Human-Centered Technology (Computer Graphics Research Division), TU Wien, Apr. 2018. Online Thesis. 2, 3

[Rhe00] RHEINGANS P. L.: Task-based color scale design. In *28th AIPR Workshop: 3D Visualization for Data Exploration and Decision Making* (2000), vol. 3905, International Society for Optics and Photonics, pp. 35–44. 3

[RMB*16] RAIDOU R., MARCELIS F., BREEUWER M., GRÖLLER M. E., VILANOVA A., VAN DE WETERING H.: Visual analytics for the exploration and assessment of segmentation errors. *Eurographics Workshop on Visual Computing for Biology and Medicine* (Sept. 2016), 193–202. 1, 4

[SBV*13] SCHADEWALDT N., BYSTROV D., VIK T., SCHULZ H., PETERS J., FRANZ A., BUERGER C., BZDUSEK K.: Robust initialization of multi-organ shape models. In *MICCAI Challenge Workshop on Segmentation: Algorithms, Theory and Applications* (2013), vol. 1, p. 3. 1

[SMS09] SILVA S., MADEIRA J., SANTOS B. S.: PolyMeCo - An integrated environment for polygonal mesh analysis and comparison. *Computers & Graphics 33*, 2 (2009), 181–191. 2

[SPA*14] SCHMIDT J., PREINER R., AUZINGER T., WIMMER M., GRÖLLER M. E., BRUCKNER S.: YMCA - Your Mesh Comparison Application. In *IEEE Visual Analytics Science and Technology* (nov 2014), VAST, IEEE Computer Society. 2

[TWSM*11] TORSNEY-WEIR T., SAAD A., MÖLLER T., HEGE H.-C., WEBER B., VERBAVATZ J.-M., BERGNER S.: Tuner: Principled parameter finding for image segmentation algorithms using visual response surface exploration. *IEEE Transactions on Visualization and Computer Graphics 17*, 12 (2011), 1892–1901. 1

[vLBB15] VON LANDESBERGER T., BASGIER D., BECKER M.: Comparative Local Quality Assessment for 3D Medical Image Segmentation with Focus on Statistical Shape Model-based Algorithms. *IEEE Transactions on Visualization and Computer Graphics* (2015). 1

[vLBK*13] VON LANDESBERGER T., BREMM S., KIRSCHNER M., WESARG S., KUIJPER A.: Visual analytics for model-based medical image segmentation: Opportunities and challenges. *Expert Systems with Applications 40*, 12 (2013), 4934 – 4943. 1

[Was15] WASHINGTON, C.M. AND LEAVER, D.T.: *Principles and Practice of Radiation Therapy.* Elsevier - Health Sciences Division, 2015. 1